Singularity removal in a quantum effective evolution of the mixmaster cosmological model

Hector Hernandez-Hernandez* and Gustavo Sanchez-Herrera†

Universidad Autonoma de Chihuahua, Facultad de Ingenieria, Nuevo Campus Universitario, Chihuahua 31125, Mexico
and Universidad Autonoma Metropolitana- Unidad Iztapalapa, Ciudad de Mexico, CDMX 09340, Mexico

(Received 17 January 2024; accepted 20 June 2024; published 5 August 2024)

In this work we analyze the evolution of the quantum mixmaster cosmological model within an effective approach. In particular, we study the behavior of the scale factor and anisotropies of the theory, and determine how it deviates from its classical counterpart due to quantum backreaction. Remarkably, we determine that the effective evolution avoids the initial singularity. The semiclassical dynamic of the system is obtained from a Hamiltonian in an extended phase space, whose classical position and momentum variables are the expectation values of the corresponding quantum operators, as well as of quantum dispersions and correlations of the system, and it is in this framework that we obtain semiclassical one-particle trajectories.

DOI: 10.1103/PhysRevD.110.043506

I. INTRODUCTION

In the mid-20th century Lifshitz discovered that as the universe shrinks to regions of space close to the initial singularity, spacetime is no longer isotropic [1]. Because of this, the interest in anisotropic cosmological models increased considerably during the past years [2–5]. One of the most prominent results of these investigations is the Belinski-Khalatnikov-Lifshitz (BKL) conjecture, stating that, in a general way, it is possible to neglect the matter terms near the initial singularity because, for them, time derivatives are dominant over those with spatial derivatives; the dynamics in this case is described by the Bianchi IX model [6]. In recent years, a great variety of studies of anisotropic models of the universe, based on this conjecture, have been carried out [7–9]. The most general anisotropic homogeneous model of the universe, based on the BKL conjecture, is the mixmaster [10]. It describes the behavior of the universe near the initial singularity. The universe is treated as a point particle moving through the anisotropies space, subject to a time-dependent potential [11]. The studies carried out on the classic mixmaster model have shown that it not only is singular but also has a chaotic behavior close to the initial singularity [12–14]; therefore, a quantization scheme is introduced in the anticipation of mitigating these issues. Among the most interesting approaches in the analysis of these quantum cosmological models are effective quantization schemes based on loop quantum gravity [15] and effective polymeric quantum mechanics [16], showing that the initial singularity is removed and the chaos present in the theory is reduced [17]. This shows the importance of effective quantization approaches in analyzing complex cosmological models, as the ones mentioned above.

Quantum effective methods in quantum mechanics allow us to obtain an approximate solution of the whole system. In particular, momenta quantum mechanics reduces quantum systems to semiclassical ones, where the dynamics is obtained from an effective Hamiltonian in an extended phase space [18]. One of the most prominent features of this method is that the notion of individual particle trajectories is recovered, a characteristic not existing in usual quantum mechanics. These trajectories describe the evolution of expected values of position and momentum operators, and of the (infinite many) quantum dispersions. The versatility of application of this method has allowed the study of a broad spectrum of quantum systems, ranging from the relatively simple phenomenon of quantum tunneling [19] to models of quantum cosmology [20–22].

In this work we obtain a system of effective equations of motion for spatial anisotropies and the scale factor of the mixmaster model, once we determine the effective extended Hamiltonian. The interaction of the several degrees of freedom of the system is encoded in an effective potential, obtained in a direct way. In Sec. II we review the more general aspects of the classical mixmaster model and perform a canonical transformation to explicitly express the Hamiltonian of the theory as a kinetic plus potential term. In Sec. III we provide the formalism of momenta quantum mechanics, and we apply this to the mixmaster model to obtain the effective dynamics of the system. Finally, in Sec. IV the semiclassical evolution is analyzed.

*Contact author: hhernandez@uach.mx
†Contact author: cbi2233805002@xanum.uam.mx

II. CLASSICAL MIXMASTER MODEL

The interest in investigating the mixmaster model lies in its representation as a general solution to Einstein's equations near the initial singularity [23]. Furthermore, various studies have been conducted that provide substantial evidence supporting the BKL conjecture [24–26]. We will analyze the quantum model with an effective prescription of quantum mechanics, so we start with a discussion of the classical model. The most general anisotropic cosmological model is the Bianchi IX, whose metric is given by [11]

$$ds^2 = -N^2dt^2 + g_{ij}\sigma_i\sigma_j, \tag{1}$$

where N is the lapse function and σ are differential forms of the three-sphere [27]

$$\begin{aligned}\sigma_1 &= \cos(\psi)d\theta + \sin(\psi)\sin(\theta)d\phi,\\ \sigma_2 &= \sin(\psi)d\theta - \cos(\psi)\sin(\theta)d\phi,\\ \sigma_3 &= d\psi + \cos(\theta)d\phi.\end{aligned}$$

In particular, the metric $g_{ij}(t)$ can be written in terms of the Misner parameters α and β such that (1) is

$$ds^2 = -N^2dt^2 + e^{2\alpha}(e^{2\beta})_{ij}\sigma^i\sigma^j, \tag{2}$$

where α is the parameter determining the volume of the universe and β_{ij} is a null trace matrix $\mathrm{tr}(\beta_{ij}) = 0$ containing the spatial anisotropies. The components of the matrix β_{ij} satisfy the following equations [28]:

$$\begin{aligned}\beta_{11} &= \beta_+ + \sqrt{3}\beta_-,\\ \beta_{22} &= \beta_+ - \sqrt{3}\beta_-,\\ \beta_{33} &= -2\beta_+,\end{aligned} \tag{3}$$

where β_+ and β_- are the shape parameters defined as [22]

$$\begin{aligned}\beta_+ &= -\frac{1}{2}\ln\left(\frac{a_3}{(a_1a_2a_3)^{1/3}}\right),\\ \beta_- &= \frac{1}{2\sqrt{3}}\ln\left(\frac{a_1}{a_2}\right),\end{aligned} \tag{4}$$

and a_1, a_2, a_3 are the scale factors in each spatial direction. On the other hand, the square root of the determinant of the metric $\sqrt{\det(g_{ij})}$ from Eq. (2) allows us to identify the volume of the universe as the scale factor $a(t)$ in terms of the parameter α [11],

$$a(t) = (a_1a_2a_3)^{1/3} = \sqrt{\det(g_{ij})} = \exp(3\alpha). \tag{5}$$

The relation between the parameters α, β_+, β_- with the scale factor $a(t)$ is [28]

$$\begin{aligned}\alpha(t) &= \frac{1}{3}\ln(a(t)),\\ \beta_+(t) &= \frac{1-P_3}{2}\alpha(t),\\ \beta_-(t) &= \sqrt{3}(P_1-P_2)\alpha(t),\end{aligned} \tag{6}$$

where P_i are the Kasner coefficients. For instance, to describe a universe that expands in two directions, and contracts in the other, the coefficients P_i are $P_1 = P_3 = 2/3$, and $P_2 = -1/3$ [29]. Equation (5) shows that as $\alpha \to -\infty$, $a(t) \to 0$, which corresponds to the initial singularity.

Once the Hamiltonian formulation for the Bianchi IX model is introduced, the resulting model is called the mixmaster. Its dynamics is determined by a Hamiltonian constraint $\mathcal{H}$, which is obtained through the variation of the following action [28]:

$$I = \int dt(p_\alpha\dot{\alpha} + p_+\dot{\beta}_+ + p_-\dot{\beta}_- - N\mathcal{H}), \tag{7}$$

where p_α and $p_\pm$ are the conjugate momenta of α and $\beta_\pm$ satisfying $\{\alpha, p_\alpha\} = \{\beta_+, p_+\} = \{\beta_-, p_-\} = 1$ [22]. $\mathcal{H}$ is defined as

$$\mathcal{H} = \frac{k}{3(8\pi)^2}e^{-3\alpha}(-p_\alpha^2 + p_+^2 + p_-^2 + \mathcal{V}) = 0, \tag{8}$$

with

$$\mathcal{V} = \frac{3(4\pi)^4}{k^2}e^{4\alpha}V(\beta_+, \beta_-), \tag{9}$$

where $k = 8\pi G$ and $V(\beta_+, \beta_-)$ is the potential corresponding to the Bianchi IX model defined as [30]

$$\begin{aligned}V(\beta_\pm) = {}& e^{-8\beta_+} - 4e^{-2\beta_+}\cosh(2\sqrt{3}\beta_-)\\ &+ 2e^{4\beta_+}[\cosh(4\sqrt{3}\beta_-) - 1].\end{aligned} \tag{10}$$

This potential is a function of anisotropies β_+, β_-, and is graphically represented by equilateral triangles that evolve in time as shown in Fig. 1. For the isotropic case the potential, $\mathcal{V} \propto e^{4\alpha}V(\beta_\pm)$, can be negative; however, for the region under study near the initial singularity where $\alpha \to -\infty$ it can be shown that the combination $p_+^2 + p_-^2 + \mathcal{V}$ is non-negative [29,30]. In general, the physical behavior of all Bianchi universes within $\mathcal{H}$ is codified in the potential term $\mathcal{V}$, as defined by Eq. (9). Each Bianchi model corresponds to a specific equipotential line [23].

The dynamics is obtained through the variation of (7) with respect to each of the variables. The variation with

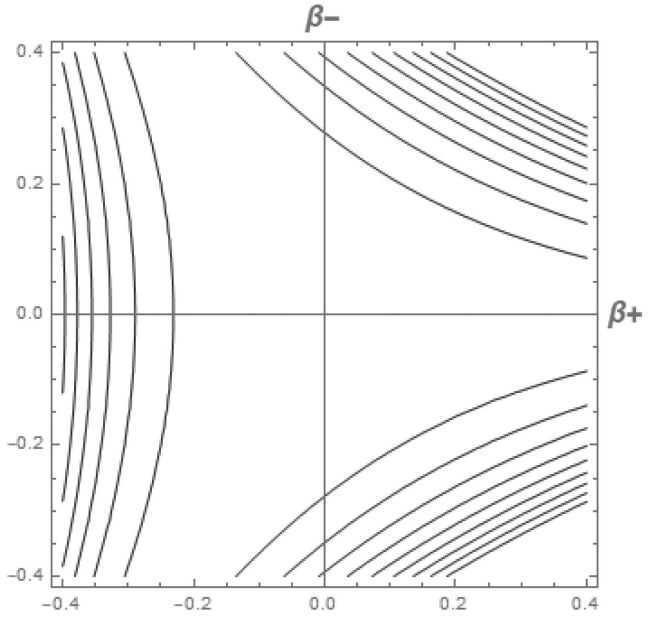

FIG. 1. Parametric representation of the mixmaster potential. Different equipotential lines correspond to different times.

respect to the lapse function N generates the Hamiltonian constraint $\mathcal{H}=0$. Solving for p_α we have

$$-p_\alpha = H_{IX} = \sqrt{p_+^2 + p_-^2 + \mathcal{V}}. \tag{11}$$

From this expression one obtains the dynamics of the universe represented as a point particle interacting with the potential (10) in the space of anisotropies (β_+,β_-) [27,30,31]. Each of the classical variables evolves with respect to the parameter α. Equations of motion are obtained from Poisson brackets between classical variables $(\beta_\pm)$ and the Hamiltonian (11). Close to the initial singularity, the particle experiences consecutive reflections as the volume of the universe decreases [28]. Near the singularity $\alpha\to-\infty$, the potential in (9) becomes negligible and the Hamiltonian is dominated only by the square root of the kinetic term. The transition time between each interaction becomes larger: oscillations take longer [22,32].

Using the Hamiltonian (11), equations of motion follow:

$$\begin{aligned}
\dot\beta_+ &= \frac{p_+}{H_{IX}},\\
\dot\beta_- &= \frac{p_-}{H_{IX}},\\
\dot p_+ &= 4\frac{3(4\pi)^2}{k^2 H_{IX}} e^{4\alpha}[e^{-8\beta_+} - e^{-2\beta_+}\cosh(2\sqrt{3}\beta_-)\\
&\quad - e^{4\beta_+}(\cosh(4\sqrt{3})-1)],\\
\dot p_- &= 4\sqrt{3}\frac{3(4\pi)^2}{k^2 H_{IX}} e^{4\alpha}[e^{-2\beta_+}\sinh(2\sqrt{3}\beta_-)\\
&\quad - e^{4\beta_+}\sinh(4\sqrt{3})].
\end{aligned} \tag{12}$$

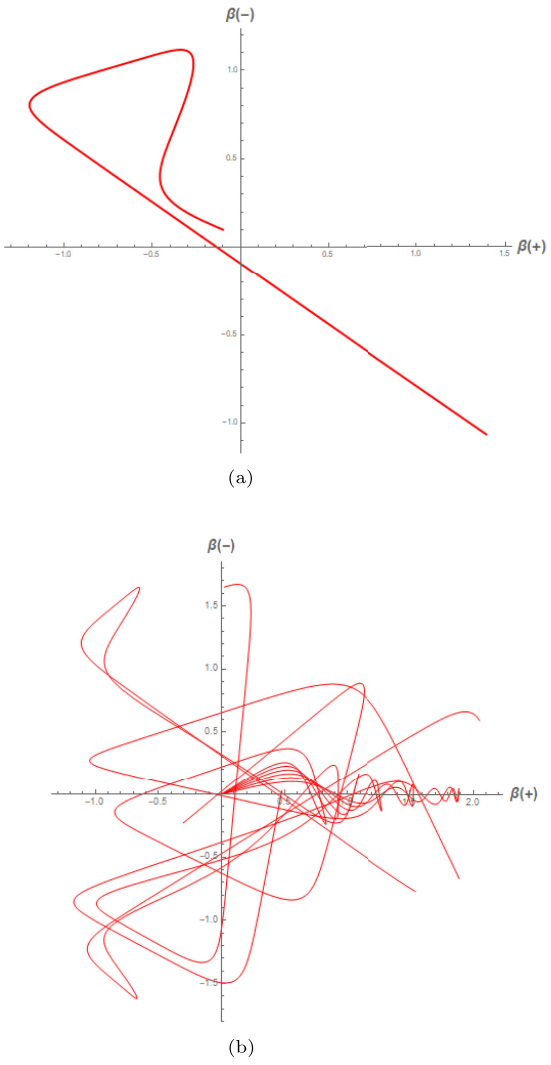

FIG. 2. Trajectory of the particle in space (β_+,β_-) for different values of $V(\beta_+,\beta_-)$. It is shown how the temporal dependence of $V(\beta_+,\beta_-)$ results in reflection in different equipotential lines. (a) Initial conditions are $\beta_+=-0.1$, $\beta_-=0.1$, $p_{\beta_+}=-3$, $p_{\beta_-}=1.28$. $V(\beta_+,\beta_-)\sim\exp\{-4\alpha\}$. (b) Initial conditions are $\beta_+=\beta_-=0$, $p_{\beta_+}=100$, $p_{\beta_-}=8$. $V(\beta_+,\beta_-)\sim\exp\{-1.2\alpha\}$.

This is a highly nonlinear, coupled system for the classical anisotropies and their momenta, so we solve it numerically. The evolution obtained is shown in Fig. 2.

Figure 2(a) shows that the trajectory of the universe experiences reflections at the potential barriers. As the particle moves away from the origin in the β_+,β_- space, the anisotropy of the model increases. Only when the particle passes through the origin where $\beta_+=\beta_-=0$ does the universe become completely isotropic. In Fig. 2(b) we show the chaotic behavior of the model by plotting different trajectories corresponding to different initial conditions.

On the other hand, in Fig. 3 we show a 3D plot in the space (α,β_+,β_-). This last simulation is similar to the one obtained in [31].

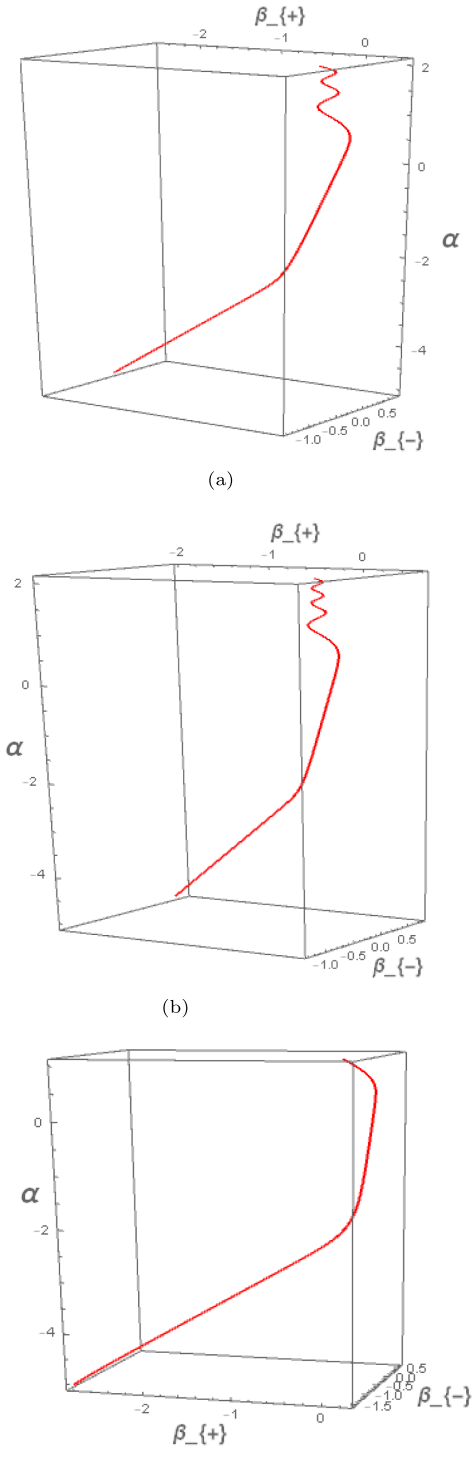

FIG. 3. Trajectory of the particle in space $(\beta_+, \beta_-, \alpha)$. The classical singularity is approached as $\alpha \to -\infty$. (a) Initial conditions are $x(0) = 0.1$, $y(0) = 0.1$, $px(0) = -60$, $py(0) = 200$. (b) Initial conditions are $x(0) = 0.1$, $y(0) = 0.1$, $px(0) = -80$, $py(0) = 200$. (c) Initial conditions are $x(0) = 0.1$, $y(0) = 0.1$, $px(0) = -30$, $py(0) = 200$.

The effective evolution above is obtained in terms of anisotropies $\beta_\pm$; to better discuss quantum modifications to the classical singularity it is useful, though, to obtain a Hamiltonian in terms of the scale factor explicitly, and to that end we consider a different expression of (11). We use the following set of variables: $q = \exp\{(3/2)\alpha\}$, $p = \frac{3}{2}\exp -\{(3/2)\alpha\}p_\alpha$ [33], and $p'_+ = p_+/q$, $\beta'_+ = \beta_+ q$, $p'_- = p_-/q$, $\beta'_- = \beta_- q$, with Poisson relations

$$\begin{aligned} \{q, p\} &= \frac{9}{4}, \\ \{\beta'_+, p'_+\} &= 1, \\ \{\beta'_+, p'_+\} &= 1. \end{aligned} \tag{13}$$

The quantization scheme following these transformations is physically well defined and can be consulted in more detail in [34]. The use of the variables defined above in the context of anisotropic cosmological models can be found in [34–38]. Using (13) it is possible to decouple the Hamiltonian (8) into a kinetic and potential term that reduces to the uncoupled Hamiltonian $\mathcal{K}$,

$$\mathcal{K} = \frac{1}{24\pi}\left(-\frac{9}{4}p^2 + p'^2_+ + p'^2_- + 12\pi^2 q^{2/3} V(q, \beta'_+, \beta'_-)\right), \tag{14}$$

where the transformed potential $V(q, \beta'_+, \beta'_-)$ is given by

$$\begin{aligned} V(q, \beta'_+, \beta'_-) = {} & e^{-\frac{8\beta'_+}{q}} - 4e^{-\frac{2\beta'_+}{q}} \cosh\left(\frac{2\sqrt{3}\beta'_-}{q}\right) \\ & + 2e^{\frac{4\beta'_+}{q}}\left[\cosh\left(\frac{4\sqrt{3}\beta'_-}{q}\right) - 1\right]. \end{aligned} \tag{15}$$

In the isotropic limit, $\beta'_+ = \beta'_- = p'_+ = p'_- = 0$, Eq. (14) becomes

$$\mathcal{K}_{\text{iso}} = -\frac{3p^2}{32\pi} - \frac{3\pi q^{2/3}}{2}, \tag{16}$$

with only 1 degree of freedom q. From this, the classical equations of motion for q and p are

$$\begin{aligned} \dot{q} &= -\frac{27}{64\pi}p, \\ \dot{p} &= \frac{9\pi}{4}q^{-1/3}. \end{aligned} \tag{17}$$

Since $q = \exp\{(3/2)\alpha\}$, from (5) we know that $q = \sqrt{a}$. Therefore, $q \to 0$ implies that $a \to 0$ and $\text{Log}(q) \to -\infty$, which corresponds to the initial singularity.

On the other hand, the equations of motion obtained from (14) are

$$\dot{q} = -\frac{27}{64\pi}p, \qquad \dot{p} = -\frac{3\pi}{4}\frac{e^{\frac{-8\beta'_+}{q}}}{q^{\frac{4}{3}}}(f-g),$$
$$\dot{\beta}'_+ = \frac{1}{12\pi}p'_+, \qquad \dot{p}'_+ = -\frac{4\pi e^{\frac{-8\beta'_+}{q}}}{q^{\frac{1}{3}}}h,$$
$$\dot{\beta}'_- = \frac{1}{12\pi}p'_-, \qquad \dot{p}'_- = \frac{4\sqrt{3}\pi e^{\frac{-2\beta'_+}{q}}}{q^{\frac{1}{3}}}j, \tag{18}$$

where f, g, h, and j are functions of q, β_+, and β_- defined as

$$f = -4e^{\frac{6\beta'_+}{q}}\left((3\beta'_+ + q)\cosh\left(\frac{2\sqrt{3}\beta'_-}{q}\right) - 3\sqrt{3}\beta'_-\sinh\left(\frac{2\sqrt{3}\beta'_-}{q}\right)\right) + (q + 12\beta'_+),$$
$$g = -2e^{\frac{12\beta'_+}{q}}\left((q-6\beta'_+)\left(1-\cosh\left(\frac{2\sqrt{3}\beta'_-}{q}\right)\right) + 6\sqrt{3}\beta'_-\sinh\left(\frac{4\sqrt{3}\beta'_-}{q}\right)\right),$$
$$h = e^{\frac{6\beta'_+}{q}}\cosh\left(\frac{2\sqrt{3}\beta'_-}{q}\right) + 2e^{\frac{12\beta'_+}{q}}\sinh^2\left(\frac{2\sqrt{3}\beta'_-}{q}\right) - 1,$$
$$j = \sinh\left(\frac{2\sqrt{3}\beta_-}{q}\right) - e^{\frac{6\beta_+}{q}}\sinh\left(\frac{4\sqrt{3}\beta_-}{q}\right). \tag{19}$$

The numerical evolution of the anisotropies β_+, β_- for the above system is shown in Fig. 4. This evolution shows a consistency with the behavior of trajectories obtained in Fig. 2. The main difference between (11) and (14) is the explicit dependence on the factor q related with the volume of the universe.

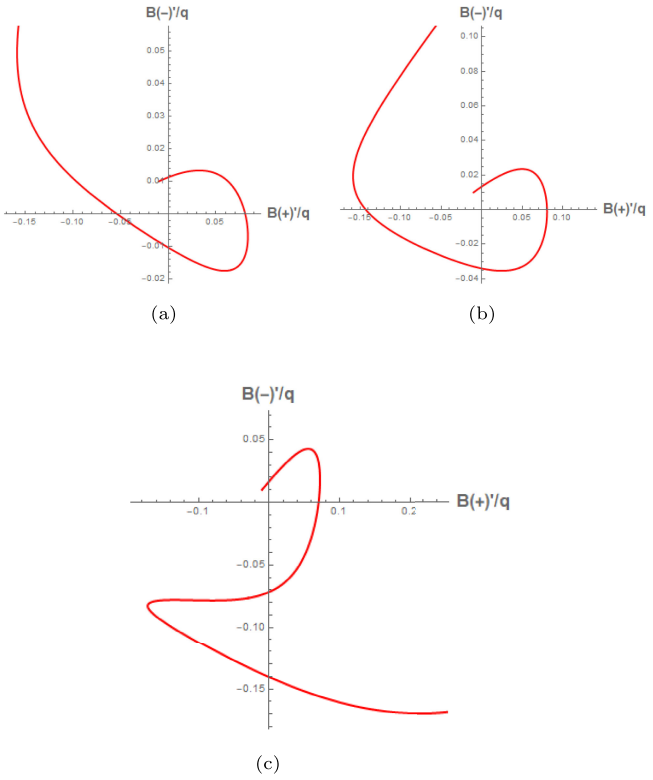

FIG. 4. Classical evolution in the space (β'_+, β'_-). (a) $q(0) = 10$, and $p(0) = 0$, $\beta'_+ = -0.1$, $\beta'_- = 0.1$, $p'_+ = 7.15$, $p'_- = 1$. (b) $q(0) = 10$, and $p(0) = 0$, $\beta'_+ = -0.1$, $\beta'_- = 0.1$, $p'_+ = 7.15$, $p'_- = 2.5$. (c) $q(0) = 10$, and $p(0) = 0$, $\beta'_+ = -0.1$, $\beta'_- = 0.1$, $p'_+ = 7.15$, $p'_- = 5$.

III. EFFECTIVE DYNAMICS OF THE MIXMASTER MODEL

A. Effective momenta quantum mechanics

In usual quantum mechanics, the Schrödinger equation determines the evolution of the system: all the information is encoded in the wave function, and classical variables are now operators. Within this Schrödinger representation, the concept of the position of a single particle is absent, therefore, trajectories that determine its evolution cannot be constructed. It is possible, however, with a generalization of the Ehrenfest theorem, to obtain an effective description by means of a Hamiltonian $H_Q = \langle\hat{H}\rangle$, which depends on expectation values of observables and quantum dispersions (or momenta) [39]. Once this Hamiltonian is obtained, dynamical equations of motion can be obtained in the usual way through the following equation:

$$\{\langle\hat{f}\rangle, \langle\hat{g}\rangle\} = \frac{1}{i\hbar}\langle[\hat{f}, \hat{g}]\rangle. \tag{20}$$

For 1 degree of freedom, these momenta are defined as

$$G^{a,b} := \langle(\hat{p} - \langle\hat{p}\rangle)^a(\hat{q} - \langle\hat{q}\rangle)^b\rangle_{\text{Weyl}}, \tag{21}$$

where $\langle\hat{q}\rangle$ and $\langle\hat{p}\rangle$ are the expectation values of position and momentum, respectively, and $a + b \geq 2$. The legend Weyl means totally symmetrization [20]. The momenta $G^{a,b}$ obey a generalization of the Heisenberg uncertainty principle [18], that is,

$$G^{2,0}G^{0,2} - (G^{1,1})^2 \geq \frac{\hbar^2}{4}. \tag{22}$$

The effective Hamiltonian H_{eff} is defined in the following way:

$$H_{\text{eff}} = \sum_{a=0}^{\infty}\sum_{b=0}^{\infty}\frac{1}{a!b!}\frac{\partial^{a+b}H}{\partial p^a \partial q^b}G^{a,b}. \tag{23}$$

A general expression for k degrees of freedom for H_{eff} is [40]

$$H_{\text{eff}} = \sum_{a_1,b_1}^{\infty} \cdots \sum_{a_k,b_k}^{\infty} \frac{1}{a_1!b_1! \cdots a_k!b_k!} \frac{\partial^{a_1+b_1+\cdots+a_k+b_k} H}{\partial q_1^{a_1} \partial p_1^{b_1} \cdots \partial q_k^{a_k} \partial p_k^{b_k}} \times G^{a_1,b_1,\ldots,a_k,b_k}. \quad (24)$$

For general systems there are an infinite number of momenta and, correspondingly, an infinite number of equations of motion, usually impossible to solve analytically, although consistent truncations can be implemented to obtain approximated solutions [41].

Analysis of this effective dynamics is done usually in a numerical way, for which initial conditions are required. We employ general squeezed states to determine such conditions; for example, for the wave function $\psi(\chi)$,

$$\psi(\chi) = \frac{1}{\pi^{1/4}\sqrt{\sigma}} \exp\left\{ -\frac{(\chi-\chi_0)^2}{2\sigma^2} + \frac{i\chi p_0}{\hbar} \right\}, \quad (25)$$

we can readily obtain the initial values for quantum variables. For instance,

$$G^{a,b} = \begin{cases} 2^{-(a+b)} \hbar^a \sigma^{b-a} \frac{a!b!}{(a/2)!(b/2)!}, & a \text{ and } b \text{ even} \\ 0, & \text{otherwise.} \end{cases} \quad (26)$$

One can see that the initial momenta $G^{a,b}$ saturate the Heisenberg uncertainty relation

$$G^{2,0}G^{0,2} = \frac{\hbar^2}{4}.$$

In this effective formulation, the momenta scale as powers of $\hbar$, that is,

$$G^{a,b} \propto \hbar^{\frac{(a+b)}{2}}.$$

It is possible to obtain important modifications of the classical system considering only the second order terms [41].

On the other hand, the momenta $G^{a,b}$ form a set of noncanonical coordinates in the quantum phase state which complicates the canonical analysis of the system [42]. However, it is possible to generalize this effective method through a coordinate transform that allows us to rewrite the momenta in terms of pairs of canonical variables s_i, p_{s_i}, and Casimir parameters [43]. These new coordinates encode all the quantum information of the system. The main advantage of this reformulation is that it avoids the truncation required by the momenta approach and allows us to construct an effective potential [44]

$$V_{\text{All}}(q,s) = \frac{1}{8s^2} + \frac{1}{2}[V(q+s) + V(q-s)], \quad (27)$$

where $V(q)$ is the classical potential of the system. In general, for 3 degrees of freedom we have [45]

$$V_{\text{All}}(x_i,s_j) = \sum_{i=1}^{3} \frac{U}{2s_i^2} + \frac{1}{8}[V(x_i+s_i) + V(x_i-s_i)]. \quad (28)$$

For a second order truncation in the momenta $G^{a,b}$ the coordinate transformation is

$$\begin{aligned} s &= \sqrt{G^{0,2}}, \\ p_s &= \frac{G^{1,1}}{\sqrt{G^{0,2}}}, \\ U &= G^{0,2}G^{2,0} - (G^{1,1})^2, \end{aligned} \quad (29)$$

where $\{s, p_s\} = 1$ and $\{s, U\} = \{p_s, U\} = 0$ [42].

B. Momenta effective dynamics for H_{IX}

To analyze the effective evolution of anisotropies β_+, β_-, we use the Hamiltonian (11)

$$H_{IX} = \sqrt{p_x^2 + p_y^2 + \frac{3(4\pi)^2}{k^2} e^{4\alpha} V(x,y)}, \quad (30)$$

where the potential $V(x,y)$ is

$$V(x,y) = e^{-8x} - 4e^{-2x}\cosh(2\sqrt{3}y) + 2e^{4x}[\cosh(4\sqrt{3}y) - 1]. \quad (31)$$

We have rewritten (for simplicity and to facilitate the numerical application of the method) $\beta_+ \to x$, $\beta_- \to y$, $p_+ \to p_x$, and $p_- \to p_y$.

Using the Hamiltonian (30), and truncating to second order in momenta Eq. (24), we obtain the following expression:

$$\begin{aligned} H_{QIX} = H_{IX} &+ (H_{IX}^{-1} - p_x^2 H_{IX}^{-3}) G^{0200} \\ &+ (H_{IX}^{-1} - p_y^2 H_{IX}^{-3}) G^{0002} + \eta \left[2\frac{\partial}{\partial x}(g_1 H_{IX}^{-1}) G^{2000} \right. \\ &+ 2\sqrt{3}\frac{\partial}{\partial y}(g_2 H_{IX}^{-1}) G^{0020} \\ &\left. - \frac{4p_x}{H_{IX}^3} g_1 G^{1100} - \frac{4\sqrt{3}p_y}{H_{IX}^3} g_2 G^{0011} \right]. \end{aligned} \quad (32)$$

The functions $g_1 = g_1(x,y)$, $g_2 = g_2(x,y)$, and $\eta = \eta(\alpha)$ are as follows:

$$\begin{aligned} g_1(x,y) &= -e^{-8x} + e^{-2x}\cosh(2\sqrt{3}y) \\ &\quad + e^{4x}(\cosh(4\sqrt{3}y) - 1), \\ g_2(x,y) &= -e^{-2x}\sinh(2\sqrt{3}y) + e^{4x}\sinh(4\sqrt{3}y), \\ \eta(\alpha) &= \frac{3(4\pi)^2}{k^2} e^{4\alpha}, \end{aligned} \quad (33)$$

and the momenta for 2 degrees of freedom are given by

$$G^{abcd} \coloneqq \langle (\hat{x} - \langle \hat{x} \rangle)^a (\hat{y} - \langle \hat{y} \rangle)^b \times (\hat{p}_x - \langle \hat{p}_x \rangle)^c (\hat{p}_y - \langle \hat{p}_y \rangle)^d \rangle_{\text{Weyl}}. \tag{34}$$

The equations of motion for the classical variables are

$$\begin{aligned}
\dot{x} &= \frac{p_x}{H_{IX}} - 2p_x\eta\frac{\partial}{\partial x}(g_1 H_{IX}^{-3})G^{2000} - 4\eta g_1\frac{\partial}{\partial p_x}(p_x H_{IX}^{-3})G^{1100} + \frac{1}{2}\frac{\partial}{\partial p_x}(H_{IX}^{-1} - p_x^2 H_{IX}^{-3})G^{0200} \\
&\quad + 2\sqrt{3}\eta\frac{\partial^2}{\partial p_x \partial_y}(g_2 H_{IX}^{-1})G^{0020} - 4\sqrt{3}p_y\eta\frac{\partial}{\partial p_x}(H_{IX}^{-3})g_2 G^{0011} + \frac{1}{2}\frac{\partial}{\partial p_x}(H_{IX}^{-1} - p_y^2 H_{IX}^{-3})G^{0002}, \\
\dot{y} &= \frac{p_y}{H_{IX}} + 2\eta\frac{\partial^2}{\partial x \partial p_y}(g_1 H_{IX}^{-1})G^{2000} - 4p_x\eta\frac{\partial}{\partial p_y}(g_1 H_{IX}^{-3})G^{1100} + \frac{1}{2}\frac{\partial}{\partial p_y}(H_{IX}^{-1} - p_x^2 H_{IX}^{-3})G^{0200} \\
&\quad + 2\sqrt{3}\eta\frac{\partial^2}{\partial p_x \partial_y}(g_2 H_{IX}^{-1})G^{0020} + \frac{\partial}{\partial y}(H_{IX}^{-1} - p_y^2 H_{IX}^{-3})G^{0011} + \frac{1}{2}\frac{\partial}{\partial p_y}(H_{IX}^{-1} - p_y^2 H_{IX}^{-3})G^{0002}, \\
\dot{p}_x &= -4\eta g_1 H_{IX}^{-1} - 2\eta\frac{\partial^2}{\partial x^2}(g_1 H_{IX}^{-1})G^{2000} - 4\eta\frac{\partial^2}{\partial x \partial p_x}(g_1 H_{IX}^{-1})G^{1100} - \frac{1}{2}\frac{\partial}{\partial x}(H_{IX}^{-1} - p_x^2 H_{IX}^{-3})G^{0200} \\
&\quad - 2\sqrt{3}\eta\frac{\partial^2}{\partial x \partial y}(g_2 H_{IX}^{-1})G^{0020} + 4\sqrt{3}p_y\eta\frac{\partial}{\partial x}(g_2 H_{IX}^{-3})G^{0011} - \frac{1}{2}\frac{\partial}{\partial x}(H_{IX}^{-1} - p_y^2 H_{IX}^{-3})G^{0002}, \\
\dot{p}_y &= -4\sqrt{3}\eta g_2 H_{IX}^{-1} - 2\eta\frac{\partial^2}{\partial x \partial y}(g_1 H_{IX}^{-1})G^{2000} + 4p_x\eta\frac{\partial}{\partial y}(g_1 H_{IX}^{-3})G^{1100} - \frac{1}{2}\frac{\partial}{\partial y}(H_{IX}^{-1} - p_x^2 H_{IX}^{-3})G^{0200} \\
&\quad - 2\sqrt{3}\eta\frac{\partial^3}{\partial y^3}(g_2 H_{IX}^{-1})G^{0020} - 4\sqrt{3}\eta\frac{\partial^2}{\partial_y \partial p_y}(g_2 H_{IX}^{-1})G^{0011} - \frac{1}{2}\frac{\partial}{\partial y}(H_{IX}^{-1} - p_y^2 H_{IX}^{-3})G^{0002},
\end{aligned} \tag{35}$$

and for the momenta,

$$\begin{aligned}
\dot{G}^{2000} &= \frac{8p_x}{H_{IX}^3}\eta g_1 G^{2000} - 2(H_{IX}^{-1} - p_x^2 H_{IX}^{-3})G^{1100}, \\
\dot{G}^{1100} &= 4\eta\frac{\partial}{\partial x}(g_1 H_{IX}^{-1})G^{2000} - (H_{IX}^{-1} - p_x^2 H_{IX}^{-3})G^{0200}, \\
\dot{G}^{0200} &= 8\eta\frac{\partial}{\partial x}(g_1 H_{IX}^{-1})G^{1100} - \frac{8p_x}{H_{IX}^3}\eta(\alpha)g_1 G^{0200}, \\
\dot{G}^{0020} &= \frac{8\sqrt{3}p_y}{H_{IX}^3}\eta g_2 G^{0020} - 2(H_{IX}^{-1} - p_y^2 H_{IX}^{-3})G^{0011}, \\
\dot{G}^{0011} &= 4\sqrt{3}\eta(\alpha)\frac{\partial}{\partial y}(g_2 H_{IX}^{-1})G^{0020} - (H_{IX}^{-1} - p_y^2 H_{IX}^{-3})G^{0002}, \\
\dot{G}^{0002} &= 8\sqrt{3}\eta\frac{\partial}{\partial y}(g_2 H_{IX}^{-1})G^{0011} - \frac{8\sqrt{3}p_y}{H_{IX}^3}\eta g_2 G^{0002}.
\end{aligned} \tag{36}$$

These are two sets of coupled and highly nonlinear equations providing the evolution of the quantum modified anisotropies, and we employ a numerical method to obtain the dynamics of this system and its trajectories.

C. Momenta effective dynamics for $\mathcal{K}_{\text{iso}}$

Using the isotropic Hamiltonian (16), and truncating to second order in momenta Eq. (24), we get the effective Hamiltonoan $\mathcal{K}_{\text{iso}}^{\text{eff}}$,

$$\mathcal{K}_{\text{iso}}^{\text{eff}} = \mathcal{K}_{\text{iso}} + \frac{3\pi}{18}q^{-4/3}G^{2,0} - \frac{1}{24\pi}G^{0,2}. \tag{37}$$

The momenta for 1 degree of freedom are

$$G^{a,b} \coloneqq \langle (\hat{q} - \langle \hat{q} \rangle)^a (\hat{p} - \langle \hat{p} \rangle)^b \rangle_{\text{Weyl}}, \tag{38}$$

and the equations of motion for the classical variables are

$$\dot{q} = -\frac{27}{64\pi}p, \qquad \dot{p} = \frac{\pi q^{-7/3}}{2}G^{2,0} + \frac{p\pi}{4}q^{-1/3}, \tag{39}$$

while for the momenta we have

$$\begin{aligned}
\dot{G}^{2,0} &= \frac{3}{8\pi}G^{1,1}, \\
\dot{G}^{1,1} &= -\frac{3}{16\pi}G^{0,2} + \frac{\pi q^{-4/3}}{3}G^{2,0}, \\
\dot{G}^{0,2} &= \frac{2\pi q^{-4/3}}{3}G^{1,1}.
\end{aligned} \tag{40}$$

D. Momenta effective dynamics for $\mathcal{K}$

The effective second order anisotropic Hamiltonian $\mathcal{K}_{\text{eff}}$ is obtained similarly using (24) for 3 degrees of freedom, and in this case $\mathcal{K}_{\text{eff}}$ is

TABLE I. Second order momenta for 3 degrees of freedom.

$A = G^{200000}$	$D = G^{002000}$	$G = G^{000020}$
$B = G^{110000}$	$E = G^{001100}$	$H = G^{000011}$
$C = G^{020000}$	$F = G^{000200}$	$J = G^{000002}$

$$\mathcal{K}_{\text{eff}} = \mathcal{K} + \frac{1}{2}\left(\frac{\partial^2\mathcal{K}}{\partial q^2}A + \frac{\partial^2\mathcal{K}}{\partial\beta'^2_+}D + \frac{\partial^2\mathcal{K}}{\partial\beta'^2_-}G\right) - \frac{3}{32\pi}C + \frac{1}{24\pi}(F+J), \tag{41}$$

where the momenta for 3 degrees of freedom are defined as follows:

$$G^{abcdef} \coloneqq \langle(\hat{q} - \langle\hat{q}\rangle)^a(\hat{\beta}'_+ - \langle\hat{\beta}'_+\rangle)^b(\hat{\beta}'_- - \langle\hat{\beta}'_-\rangle)^c \times (\hat{p} - \langle\hat{p}\rangle)^d(\hat{p}'_+ - \langle\hat{p}'_+\rangle)^e(\hat{p}'_- - \langle\hat{p}'_-\rangle)^f\rangle_{\text{Weyl}}. \tag{42}$$

In Table I, the second order momenta are summarized. The equations of motion obtained from (41) form a system of 15 coupled equations that describe the dynamics of the mixmaster model. Equations for the classical variables are

$$\begin{aligned}
\dot{p} &= -\frac{\partial\mathcal{K}}{\partial q} - \frac{1}{2}\left(\frac{\partial^3\mathcal{K}}{\partial q^3}A + \frac{\partial^3\mathcal{K}}{\partial q\partial\beta'^2_+}D + \frac{\partial^3\mathcal{K}}{\partial q\partial\beta'^2_-}G\right),\\
\dot{p}'_+ &= -\frac{\partial\mathcal{K}}{\partial\beta'_+} - \frac{1}{2}\left(\frac{\partial^3\mathcal{K}}{\partial\beta'_+\partial q^2}A + \frac{\partial^3\mathcal{K}}{\partial\beta'^3_+}D + \frac{\partial^3\mathcal{K}}{\partial\beta'_+\partial\beta'^2_-}G\right),\\
\dot{p}'_- &= -\frac{\partial\mathcal{K}}{\partial\beta'_-} - \frac{1}{2}\left(\frac{\partial^3\mathcal{K}}{\partial\beta'_-\partial q^2}A + \frac{\partial^3\mathcal{K}}{\partial\beta'_-\partial\beta'^2_+}D + \frac{\partial^3\mathcal{K}}{\partial\beta'^3_-}G\right),\\
\dot{q} &= -\frac{27}{64\pi}p,\\
\dot{\beta}'_+ &= \frac{1}{12\pi}p'_+,\\
\dot{\beta}'_- &= \frac{1}{12\pi}p'_-,
\end{aligned} \tag{43}$$

while for quantum variables we have

$$\begin{aligned}
&\dot{A} = \frac{3}{8\pi}B, \quad \dot{B} = \frac{\partial^2\mathcal{K}}{\partial q^2}A + \frac{3}{16\pi}C, \quad \dot{C} = 2\frac{\partial^2\mathcal{K}}{\partial q^2}B,\\
&\dot{D} = -\frac{1}{6\pi}E, \quad \dot{E} = \frac{\partial^2\mathcal{K}}{\partial\beta'^2_+}D - \frac{1}{12\pi}F, \quad \dot{F} = 2\frac{\partial^2\mathcal{K}}{\partial\beta'^2_+}E,\\
&\dot{G} = -\frac{1}{6\pi}H, \quad \dot{H} = \frac{\partial^2\mathcal{K}}{\partial\beta'^2_-}G - \frac{1}{12\pi}J, \quad \dot{J} = 2\frac{\partial^2\mathcal{K}}{\partial\beta'^2_-}H.
\end{aligned} \tag{44}$$

IV. NUMERICAL SOLUTION

For 1 degree of freedom, the momenta $G^{a,b}$ are defined as

$$G^{a,b} \coloneqq \langle(\hat{q} - q)^a(\hat{p} - p)^b\rangle_{\text{Weyl}},$$

where $p \coloneqq \langle\hat{p}\rangle$ and $q \coloneqq \langle\hat{q}\rangle$. Using the squeezed state (25), the initial conditions for the momenta $G^{a,b}$ can be determined. For instance, for $G^{2,0}$ we get

$$\begin{aligned}
G^{2,0} &= \langle\psi(\chi)^*|(\hat{p} - p)^2|\psi(\chi)\rangle\\
&= -\frac{\eta}{\sigma^4}\int_{-\infty}^{\infty} e^{\frac{-(\chi-\chi_0)^2}{\sigma^2}}(\zeta - 2\chi_0 * \chi + \chi^2)d\chi\\
&= \frac{\hbar^2}{2\sigma^2},
\end{aligned} \tag{45}$$

where $\eta = \frac{-\hbar^2}{\sqrt{\pi}\sigma^5}$ and $\zeta = \chi_0^2 - \sigma^2$ are constants. Following a similar procedure, the second order initial values for momenta are

$$G^{2,0} = \frac{\hbar^2}{2\sigma^2}, \qquad G^{1,1} = 0, \qquad G^{0,2} = \frac{\sigma^2}{2}. \tag{46}$$

For 2 degrees of freedom the momenta G^{abcd} are defined as

$$G^{abcd} \coloneqq \langle(\hat{p}_1 - p_1)^a(\hat{q}_1 - q_1)^b \times (\hat{p}_2 - p_2)^c(\hat{q}_2 - q_2)^d\rangle_{\text{Weyl}},$$

where $p_1 \coloneqq \langle\hat{p}_1\rangle, q_1 \coloneqq \langle\hat{q}_1\rangle, p_2 \coloneqq \langle\hat{p}_2\rangle$, and $q_2 \coloneqq \langle\hat{p}_2\rangle$. Employing a similar procedure for the 1 degree of freedom case, the initial conditions for the second order moments, with 2 degrees of freedom G^{abcd} are

$$\begin{aligned}
G^{2000} &= G^{0020} = \frac{\hbar^2}{2\sigma^2},\\
G^{1100} &= G^{0011} = 0,\\
G^{0200} &= G^{0002} = \frac{\sigma^2}{2}.
\end{aligned} \tag{47}$$

For 3 degrees of freedom we get

$$\begin{aligned}
G^{200000} &= G^{002000} = G^{000020} = \frac{\hbar^2}{2\sigma^2},\\
G^{110000} &= G^{001100} = G^{000011} = 0,\\
G^{020000} &= G^{000200} = G^{000002} = \frac{\sigma^2}{2}.
\end{aligned} \tag{48}$$

The set of equations (35) and (36) describes the dynamics of anisotropies and quantum momenta of the mixmaster model. The coupling between both kinds of variables generates a quantum backreaction that modifies the classical evolution of the system, which we explore now.

We employ initial conditions (47) to generate, numerically, the evolution of the system. In Fig. 5 we show the modification of the classical trajectories (red curves) due to the quantum effects. In Fig. 5(a) the black dot denotes the starting point of both trajectories classical and effective (green curvs), while the purple dots correspond to both trajectories at the same time. However, unlike the straight line behavior of classical trajectories near the initial singularity as $|\beta_{\pm}| \to \infty$, as discussed in Sec. II and shown in Fig. 2(a), the interaction of the quantum momenta with the classical system increases the changes in direction of the trajectory for the semiclassical particle at early times, drastically changing its linear behavior. Figure 5(b) represents the same trajectories for different evolution times.

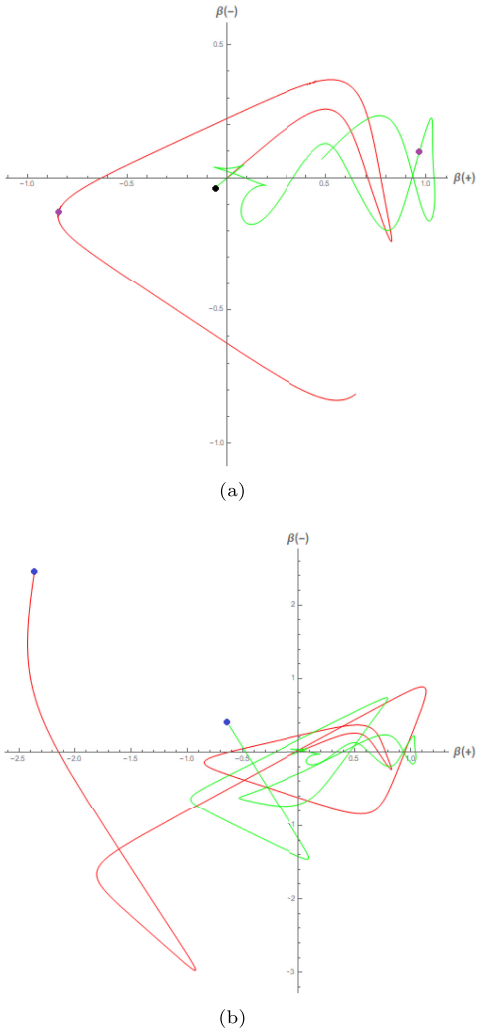

FIG. 5. Comparison between classical (red curves) and effective evolution (green curves) for the anisotropies of the mixmaster model. The dots represent the position at equal times. Initial conditions are $\beta_+(0) = 0$, $\beta_- = 0$, $p_+ = 100$, $p_- = 64$, and $\sigma = 2.2$. (a) Classical (red) and effective evolution (green) for anisotropies up to $t = 6$. (b) Classical (red) and effective evolution (green) for the anisotropies up to $t = 20$.

In Fig. 6 we show a comparison between several classical and semiclassical trajectories, displaying chaotic behavior [17]. The plots show how effective trajectories are drastically modified due to quantum backreaction, although the system retains its chaotic behavior.

In Fig. 7 we show the semiclassical evolution obtained from the effective Hamiltonian (37) for an isotropic universe. The variable q is related to the scale factor through $q = \sqrt{a}$. In this diagram the singularity is reached when $\mathrm{Log}(q) \to -\infty$, that is, $a \to 0$. The image shows the removal of the initial singularity and a bounce of the trajectories generated by the quantum momenta. As the volume of the universe decreases, the potential reaches a maximum point and subsequently decreases. After the rebound of the universe, the momentum increases again. The different colors correspond to different values of the dispersion σ.

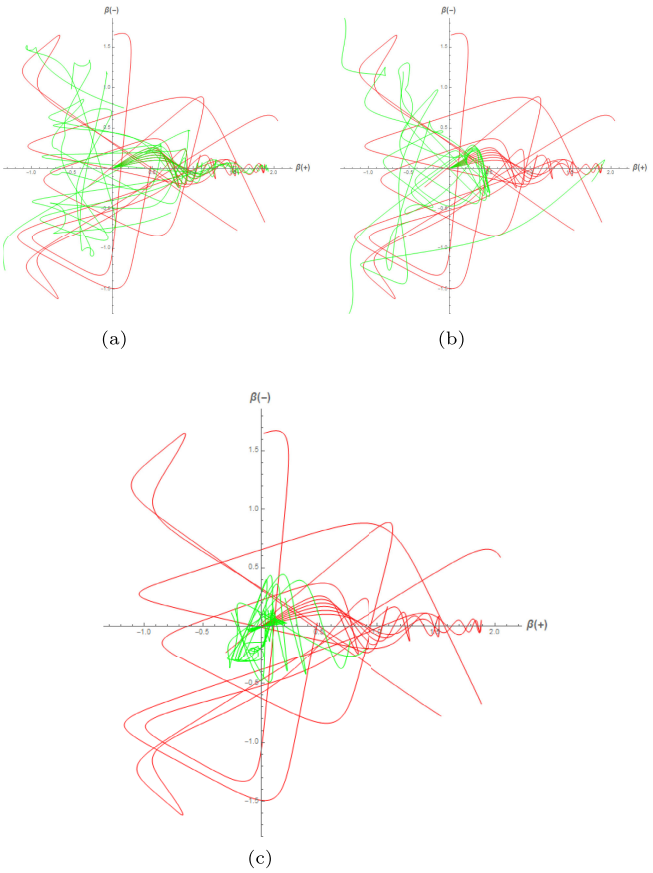

FIG. 6. Comparison between classical (red curves) and effective evolution (green curves) for the anisotropies of the mixmaster model. Initial conditions for the classical model are $\beta_+(0) = 0$, $\beta_- = 0$, $p_+ = 100$, and $p_- = 8i$ ($i = 1, 2, 3, \ldots, 10$ labels different trajectory). Initial conditions for the effective evolution are $\beta_+(0) = 0$, $\beta_- = 0$, $p_+ = 100$, and $p_- = 8i$. (a) Classical and quantum evolution for $\sigma = 0.08$. (b) Classical and quantum evolution for $\sigma = 0.6$. (c) Classical and quantum evolution for $\sigma = 2.6$.

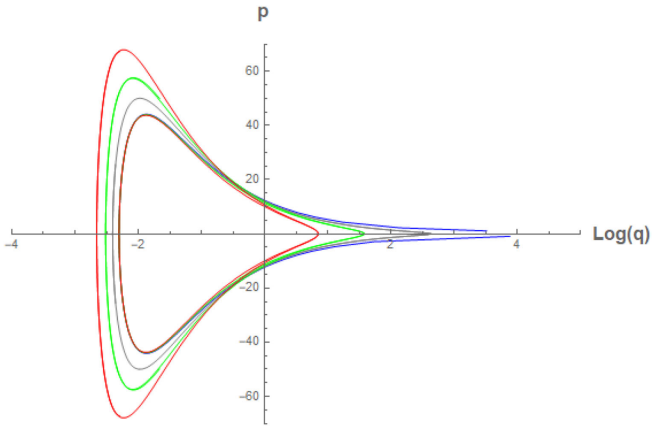

FIG. 7. Effective evolution corresponding to the isotropic Hamiltonian (37). The graph shows the removal of the initial singularity through the rebound of the effective trajectories. Different colors correspond to different values of σ. Initial conditions are $q(0) = 10$, $p(0) = 0$ and $\sigma = 0.5$, $\sigma = 4$, $\sigma = 8$, and $\sigma = 13$.

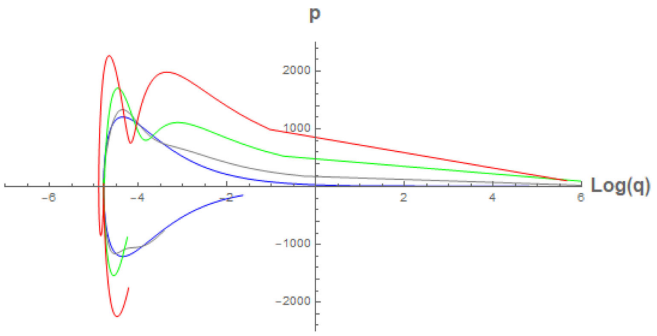

FIG. 8. Effective evolution corresponding to the anisotropic Hamiltonian (41). The graph shows the removal of the initial singularity through the rebound of the effective trajectories. Different colors correspond to different values of σ. Initial conditions are $q(0) = 120$, $p(0) = 0$, $\beta'_+(0) = 0.01$, $p_+(0) = 0$, $\beta'_-(0) = 0.05$, $p_-(0) = 0$, and $\sigma = 3$, $\sigma = 25$, $\sigma = 50$, and $\sigma = 75$.

Finally, in Fig. 8 we show again the removal of the initial singularity in an anisotropic universe for different values of the dispersion σ. We can see that the effective model is highly susceptible to small changes in the initial conditions corresponding to anisotropies. These small variations of β_+ and β_- have important implications on the behavior of the momentum p. The results obtained corresponding to the removal of the singularity for the anisotropic model are similar to those obtained in [33,37].

V. CONCLUSIONS

In this article the quantum mixmaster model was analyzed in a semiclassical setting, finding important differences with respect to the classical model. In particular, by studying semiclassical trajectories describing the evolution of anisotropies we show that the initial singularity is avoided as a result of quantum backreaction.

In the classical mixmaster model, the universe interacts with a time-dependent potential evolving in a space of anisotropies, where the interaction with the potential walls is less frequent as we approach the singularity. The classical evolution was obtained through numerical simulations and displayed in Figs. 2 and 3, matching those obtained in [46–48]. We apply a transformation from the variables α and p_α to the pair q and p in the classical Hamiltonian to obtain an expression in terms of the scale factor. Under this formulation it is possible to make a direct comparison between the quantum corrected behavior and that of the classical model by means of effective trajectories.

The behavior displayed by the quantum model derived from the effective Hamiltonian (32) shows that, although the classical evolution is drastically modified due to quantum backreaction through quantum momenta, it retains its chaotic behavior regardless of initial conditions taken into account, in agreement with recent similar studies [17].

In the classical evolution, as we reach the initial singularity we get $|\beta_\pm| \to \infty$, and the particle experiences an infinite number of reflections, less frequent each time. In the quantum regime, the interaction of the particle with the potential is stronger due to backreaction, generating more dispersions and preventing the particle from reaching $|\beta_\pm| \to \infty$, effectively avoiding the singularity.

We obtain two effective Hamiltonians, one corresponding to the isotropic limit in terms of the scale factor $a(t)$ (37) and another for the anisotropic model (41) as a function of the shape parameters β_+, β_-, and $a(t)$. In both representations it is possible to observe the removal of the initial singularity (Figs. 7 and 8). The effective equations obtained from these Hamiltonians allow us to analyze the backreaction to the scale factor and the anisotropies. The dynamics of the isotropic model (39), (40) shows a coupling between the classical variables (q, p) and the quantum momenta $G^{a,b}$. This coupling is responsible for the deviation of the effective trajectories with respect to the classical ones resulting in the removal of the singularity. In the anisotropic model the effective equations (43) and (44) become more complicated because 2 extra degrees of freedom are included corresponding to the shape parameters (β_+, β_-). In this case the momenta couple not only with the pair (q, p) but also with the anisotropies. As a consequence, the effective evolution of the scale factor is not only modified by the backreaction of the quantum variables but now the anisotropies also influence the behavior of the effective trajectory. Figure 8 shows that small variations in the shape parameters result in important modifications in the momentum of the system. These results can be comparable with those obtained in [33]. In regions where the quantum effects are negligible, that is, the momenta G^{abcd} become zero, we recover the classical dynamics of the mixmaster model.

These effective descriptions show that the quantum regime imposes a minimum lower bound on the volume of the universe.

In principle, it is possible to apply the effective potential of Eq. (28) and directly modify the Hamiltonians of Eqs. (14) and (16) to obtain an effective system. However, this requires a deeper analysis of the effective equations as well as the numerical methods to solve them. This can lead us to interesting results that can be compared with those obtained in this research work. Our study can be used to generalize the analysis of anisotropic cosmological models into inhomogeneous models, where we expect to obtain interesting results in this effective description [21,49,50].

ACKNOWLEDGMENTS

G. S. was funded by CONAHCYT scholarship 2020-000013-01NACF-05710. This work was partially supported by CONAHCYT Grant CBF-2023-2024-1937.

[1] Evgeny M. Lifshitz and Isaak M. Khalatnikov, Investigations in relativistic cosmology, Adv. Phys. **12**, 185 (1963).
[2] Alexey S. Koshelev, João Marto, and Anupam Mazumdar, Towards resolution of anisotropic cosmological singularity in infinite derivative gravity, J. Cosmol. Astropart. Phys. 02 (2019) 020.
[3] Alexey Toporensky and Shinji Tsujikawa, Nature of singularities in anisotropic string cosmology, Phys. Rev. D **65**, 123509 (2002).
[4] Bijan Saha, Anisotropic cosmological models with a perfect fluid and a λ term, Astrophys. Space Sci. **302**, 83 (2006).
[5] Burak Himmetoglu, Carlo R. Contaldi, and Marco Peloso, Instability of anisotropic cosmological solutions supported by vector fields, Phys. Rev. Lett. **102**, 111301 (2009).
[6] Hans Ringström, The bianchi ix attractor, Ann. Henri Poincaré **2**, 405 (2001).
[7] W. Piechocki, Quantum chaos of the Belinski–Khalatnikov–Lifshitz scenario, Acta Physica Polonica Supplement **16**, 21 (2023).
[8] Joshua Ritchie, Bianchi i 'asymptotically Kasner'solutions of the Einstein scalar field equations, Classical Quantum Gravity **39**, 135007 (2022).
[9] Ana Alonso-Serrano, David Brizuela, and Sara F. Uria, Quantum Kasner transition in a locally rotationally symmetric Bianchi II universe, Phys. Rev. D **104**, 024006 (2021).
[10] Eleonora Giovannetti and Giovanni Montani, Polymer representation of the Bianchi IX cosmology in the Misner variables, Phys. Rev. D **100**, 104058 (2019).
[11] Charles W. Misner, The Mixmaster cosmological metrics, *Deterministic Chaos in General Relativity* (Springer, Boston, 1994), pp. 317–328.
[12] Neil J. Cornish and Janna J. Levin, The mixmaster universe is chaotic, Phys. Rev. Lett. **78**, 998 (1997).
[13] John D. Barrow, Chaotic behaviour in general relativity, Phys. Rep. **85**, 1 (1982).
[14] Andrew Zardecki, Modeling in chaotic relativity, Phys. Rev. D **28**, 1235 (1983).
[15] Johannes Brunnemann and Thomas Thiemann, On (cosmological) singularity avoidance in loop quantum gravity, Classical Quantum Gravity **23**, 1395 (2006).
[16] Orchidea Maria Lecian, Giovanni Montani, and Riccardo Moriconi, Semiclassical and quantum behavior of the Mixmaster model in the polymer approach, Phys. Rev. D **88**, 103511 (2013).
[17] Martin Bojowald, David Brizuela, Paula Calizaya Cabrera, and Sara F. Uria, The chaotic behavior of the Bianchi IX model under the influence of quantum effects, Phys. Rev. D **109**, 044038 (2024).
[18] Martin Bojowald and Aureliano Skirzewski, Effective equations of motion for quantum systems, Rev. Math. Phys. **18**, 713 (2006).
[19] L. Aragón-Muñoz, G. Chacón-Acosta, and H. Hernandez-Hernandez, Effective quantum tunneling from a semiclassical momentous approach, Int. J. Mod. Phys. B **34**, 2050271 (2020).
[20] Martin Bojowald, David Brizuela, Hector H. Hernández, Michael J. Koop, and Hugo A. Morales-Técotl, High-order quantum back-reaction and quantum cosmology with a positive cosmological constant, Phys. Rev. D **84**, 043514 (2011).
[21] David Brizuela and Unai Muniain, A moment approach to compute quantum-gravity effects in the primordial universe, J. Cosmol. Astropart. Phys. 04 (2019) 016.
[22] David Brizuela and Sara F. Uria, Semiclassical study of the Mixmaster model: The quantum Kasner map, Phys. Rev. D **106**, 064051 (2022).
[23] Marco Valerio Battisti and Giovanni Montani, The mixmaster universe in a generalized uncertainty principle framework, Phys. Lett. B **681**, 179 (2009).
[24] Jun-Qi Guo, Daoyan Wang, and Andrei V. Frolov, Spherical collapse in f (r) gravity and the Belinskii-Khalatnikov-Lifshitz conjecture, Phys. Rev. D **90**, 024017 (2014).
[25] J. Mark Heinzle, Claes Uggla, and Woei Chet Lim, Spike oscillations, Phys. Rev. D **86**, 104049 (2012).
[26] Abhay Ashtekar, Adam Henderson, and David Sloan, Hamiltonian formulation of the Belinskii-Khalatnikov-Lifshitz conjecture, Phys. Rev. D **83**, 084024 (2011).
[27] Charles W. Misner, Mixmaster universe, Phys. Rev. Lett. **22**, 1071 (1969).
[28] Riccardo Moriconi, Salvatore Capozziello, and Giovanni Montani, Dynamical systems in quantum cosmology UNINA/ FEDOA, 10.6093/unina/fedoa/11521.
[29] Kip S. Thorne, Charles W. Misner, and John Archibald Wheeler, *Gravitation* (Freeman, San Francisco, 2000).

[30] Michael P. Ryan and Lawrence C. Shepley, *Homogeneous Relativistic Cosmologies* (Princeton University Press, Princeton, NJ, 2015).
[31] Edward Wilson-Ewing, A quantum gravity extension to the Mixmaster dynamics, Classical Quantum Gravity **36**, 195002 (2019).
[32] Martin Bojowald, David Brizuela, Paula Calizaya Cabrera, and Sara F. Uria, Chaotic behavior of the Bianchi IX model under the influence of quantum effects, Phys. Rev. D **109**, 044038 (2024).
[33] Jaime de Cabo Martín, Mixmaster universe: Semiclassical dynamics and inflation from bouncing, Acta Phys. Pol. B Proc. Suppl. **16**, A2 (2023).
[34] Hervé Bergeron, Andrea Dapor, Jean Pierre Gazeau, and Przemysław Małkiewicz, Smooth big bounce from affine quantization, Phys. Rev. D **89**, 083522 (2014).
[35] Hervé Bergeron, Ewa Czuchry, Jean-Pierre Gazeau, and Przemysław Małkiewicz, Nonadiabatic bounce and an inflationary phase in the quantum mixmaster universe, Phys. Rev. D **93**, 124053 (2016).
[36] Hervé Bergeron, Ewa Czuchry, Jean-Pierre Gazeau, Przemysław Małkiewicz, and Włodzimierz Piechocki, Smooth quantum dynamics of the mixmaster universe, Phys. Rev. D **92**, 061302 (2015).
[37] Hervé Bergeron, Ewa Czuchry, Jean-Pierre Gazeau, Przemysław Małkiewicz, and Włodzimierz Piechocki, Singularity avoidance in a quantum model of the mixmaster universe, Phys. Rev. D **92**, 124018 (2015).
[38] Hervé Bergeron, Ewa Czuchry, Jean-Pierre Gazeau, and Przemysław Małkiewicz, Vibronic framework for quantum mixmaster universe, Phys. Rev. D **93**, 064080 (2016).
[39] Martin Bojowald, *Quantum Cosmology: A Fundamental Description of the Universe* (Springer Science & Business Media, New York, 2011), Vol. 835.
[40] Hector H. Hernandez Hernandez and Carlos R. Javier Valdez, Semiclassical trajectories in the double-slit experiment, arXiv:2106.03280.
[41] Martin Bojowald, Quantum cosmology: Effective theory, Classical Quantum Gravity **29**, 213001 (2012).
[42] Ding Ding, Effective methods in cosmology and gravity, 2022.
[43] Bekir Baytaş, Martin Bojowald, and Sean Crowe, Faithful realizations of semiclassical truncations, Ann. Phys. (Amsterdam) **420**, 168247 (2020).
[44] Bekir Baytaş, Martin Bojowald, and Sean Crowe, Effective potentials from semiclassical truncations, Phys. Rev. A **99**, 042114 (2019).
[45] Bekir Baytaş, Martin Bojowald, and Sean Crowe, Canonical tunneling time in ionization experiments, Phys. Rev. A **98**, 063417 (2018).
[46] B. K. Berger, Numerical study of initially expanding mixmaster universes, Classical Quantum Gravity **7**, 203 (1990).
[47] Beverly K. Berger, Comments on the computation of Liapunov exponents for the mixmaster universe, Gen. Relativ. Gravit. **23**, 1385 (1991).
[48] Beverly K. Berger, Numerical approaches to spacetime singularities, Living Rev. Relativity **5**, 1 (2002).
[49] Martin Bojowald and Ding Ding, Canonical description of cosmological backreaction, J. Cosmol. Astropart. Phys. 03 (2021) 083.
[50] Martin Bojowald and Freddy Hancock, Quasiclassical model of inhomogeneous cosmology, Classical Quantum Gravity **40**, 155012 (2022).